JOURNAL OF AGRICULTURAL AND FOOD CHEMISTRY

Novel Secoiridoids with Antioxidant Activity from Australian Olive Mill Waste

HASSAN K. OBIED,† PETER KARUSO,‡ PAUL D. PRENZLER,† AND KEVIN ROBARDS*,†

E. H. Graham Centre for Agricultural Innovation, School of Science and Technology, Charles Sturt University, Wagga Wagga, NSW 2678, Australia, and Department of Chemistry and Biomolecular Sciences, Macquarie University, Sydney, NSW 2109, Australia

A new biophenolic secoiridoid was identified in Australian Frantoio olive mill waste (OMW) extracts. Isolation, purification, and structure elucidation were performed. Hydroxytyrosyl acyclodihydroelenolate, the first nonaldehydic acyclic secoiridoid, is reported. A second compound was identified as *p*-coumaroyl-6′-secologanoside (comselogoside), and although it has been identified recently in OMW and leaves, this is the first time it has been identified in both OMW and olive fruits. UV, mass spectral, and NMR data are given for both compounds. The two compounds were quantified by HPLC-DAD, and their antioxidant potential was assessed against the classical olive biophenols, hydroxytyrosol and oleuropein, by the in vitro DPPH radical scavenging assay.

KEYWORDS: Secologanoside; hydroxytyrosol; oleuropein; *p*-coumaric acid derivative; NMR; LC-MS; DPPH

INTRODUCTION

There has been intense interest in the biophenols extracted from olive. This can be attributed to the association of these compounds with various bioactivities (*1*−*3*). Olive biophenols are now recognized as potential nutraceutical targets for the food and pharmaceutical industries (*3*−*5*). For example, oleocanthal, the dialdehydic form of deacetoxyligstroside aglycone, is found in olives and dose-dependently inhibits COX-1 and COX-2 activities, similar to nonsteroidal anti-inflammatory drugs such as ibuprofen (*6*). The majority of the olive crop is used for oil production, resulting in the generation of large quantities of waste. Modern two-phase mills consume little or no water, and in this case the waste is mainly solid in nature, commonly described as alperujo or pomace. This study focuses on two-phase mill waste as this is the main waste-stream from Australian mills. Olive mill waste (OMW) will be used exclusively to refer to the waste generated from a two-phase processing system. The phenolic fraction of the oil comprises only 2% of the total phenolic content of the olive fruits, with the remaining 98% being lost in the OMW (*7*). Coupled with the increased production of olive oil in Australia and the accumulation of olive waste, we have viewed this waste as a potential resource and source of valuable natural products and products for biotechnology and complementary medicine (*8*). This paper describes the structure elucidation of two new biophenols from OMW based principally on nuclear magnetic resonance (NMR) spectroscopy. The antioxidant activity of these novel compounds was compared with other olive biophenols using the 2,2-diphenyl-1-picrylhydrazyl radical (DPPH•) scavenging assay (*9*).

MATERIALS AND METHODS

Olive Mill Waste. Frantoio fruit, 90% black skin coloration, was processed at Riverina Olive Grove, Wagga Wagga, Australia, in May 2003 using a commercial two-phase olive oil mill (Pieralisi, Italy) and a malaxation time and temperature of 1 h and 20 ± 1 °C, respectively (*8*). The fresh waste was stored under liquid nitrogen without delay and then freeze-dried in a Dynavac FD12 freeze-dryer (Sydney, Australia). The freeze-dried OMW was stored in screw-capped amber-colored glass containers at −20 °C. The weight of the freeze-dried OMW powder was taken as the dry weight. Gross properties of the waste have been reported elsewhere (*8*).

Recovery of Target Compounds. Freeze-dried powder (7 g) was extracted with extraction solvent (methanol/water/HCl 80+20+1 v/v/v; 40 mL) for 30 min at ambient temperature (20 ± 2 °C). After filtration, the raffinate was re-extracted with 30 mL of the same extraction solvent for 15 min and filtered over the first filtrate. The combined filtrate was defatted twice with *n*-hexane (40 mL × 2). The defatted extract was concentrated in a rotary evaporator for 30 min (at <35 °C), reconstituted with 10 mL of methanol/water/acetic acid (31:69:1, v/v/v), and saturated with sodium chloride before being filtered through GF/F filter. The filtrate was extracted with ethyl acetate (15 mL × 4), and the combined extract was dried over anhydrous sodium sulfate before removal of ethyl acetate under vacuum at <35 °C. The residue was reconstituted in methanol/water/acetic acid (31:69:1, v/v/v) and filtered through a 0.45 μm PTFE syringe filter. The ethyl acetate extract was unstable, showing decreased recovery of biophenols, particularly hydroxytyrosol acyclodihydroelenolate, even when stored at 4 °C, so evaporation and reconstitution were performed without delay.

* Corresponding author (telephone +61-2-6933-2547; fax +61-2-6933-2737; e-mail krobards@csu.edu.au).
† Charles Sturt University.
‡ Macquarie University.

10.1021/jf063300u CCC: $37.00
Published on Web 03/21/2007

Fractionation. Strata-X GIGA SPE tubes (1 g, 12 mL) (Phenomenex, Lane Cove, Australia) were conditioned with 20 mL of methanol and then equilibrated with 20 mL of water/acetic acid (100:1, v/v). Samples were loaded, and the SPE tube was washed with 30 mL of methanol/water/acetic acid (31:69:1, v/v/v). The fraction containing compound **A** was eluted with 25 mL of methanol/water/acetic acid (45:55:1, v/v/v). A wash step with 30 mL of methanol/water/acetic acid (51:50:1, v/v/v) was applied before elution of the fraction containing compound **B** with 25 mL of methanol/water/acetic acid (62:38:1, v/v/v). The flow rate throughout the whole SPE elution experiment was kept at ca. 2 mL/min by adjusting the applied vacuum. Subsequently, removal of organic solvent was performed under vacuum at <35 °C, and the aqueous residues were freeze-dried.

The process was monitored with analytical-scale HPLC as previously described (*8*). This involved gradient elution using aqueous methanol and a mixture of methanol, acetonitrile, and acetic acid at a flow rate of 1 mL/min using a 150 mm × 4.6 mm i.d., 5 μm, Luna C-18(2) column (Phenomenex).

Purification. The freeze-dried fractions were reconstituted with 80% methanol and filtered through 0.2 μm syringe nylon filter (Phenomenex). Separation, isolation, and purification of the filtered and reconstituted SPE fractions were performed using semipreparative HPLC. The system comprised a Perkin-Elmer binary LC-pump 250, ProStar 325 UV−vis detector (Varian, Palo Alto, CA) with preparative dual path flow cell, 9 mm × 1 mm, and a Varian 9300 autosampler (Varian) with a 1000 μL sample loop. Fractionation was performed on a 250 × 10 mm i.d., 5 μm, Alltima C18 column connected to a 33 × 7 mm i.d., 10 μm, Alltima Prep-Guard C18 guard column. Varian Star 6.2 software was used to control the autosampler and the UV−vis detector (280 nm). For the isolation of compound **A**, solvent A was water/methanol (95:5, v/v) and solvent B was methanol/acetonitrile (50:50, v/v). A stepwise linear gradient elution at a constant flow rate of 5 mL/min was performed for a total run time of 25 min as follows: starting from 75% solvent A and 25% solvent B, isocratic elution was performed for 3 min and then increased to 30% solvent B over 3 min, again isocratic for 9 min, increased to 35% solvent B over 5 min, and finally increased to 80% solvent B over 5 min. A different gradient program at a constant flow rate of 4.5 mL/min was used for the isolation of compound **B**: starting from 70% solvent A and 30% solvent B, isocratic elution was performed for 5 min and then increased to 35% solvent B over 5 min, again isocratic for 5 min, increased to 60% solvent B over 5 min, and returned to 30% solvent B over 5 min. Eluents were once again monitored by analytical-scale HPLC.

The collected fractions were concentrated under vacuum at 37 °C for 45 min to remove the organic solvents. The aqueous residues were freeze-dried and stored at −20 °C in airtight, amber glass containers until required. The isolated compounds showed a single major peak (ca. 70%) in their HPLC chromatograms at 278 nm. Further purification via semipreparative HPLC as before, except that solvent A was water and solvent B was acetonitrile, yielded peaks that were chromatographically at least 90% pure.

Liquid Chromatography−Mass Spectrometry (LC-MS). Samples were analyzed using a Beckman (Fullerton, CA) liquid chromatograph comprising a 126 pump and a 168 diode array detector coupled to a Quattro II mass spectrometer [Micromass (Waters), Manchester, U.K.]. The same column and conditions used for analytical-scale HPLC were used for LC-MS except for replacement of acetic acid by formic acid in the mobile phase (*8*). The eluent was split such that 150 μL min^{-1} of the flow was directed to the electrospray source. Mass spectrometric scans were performed in both positive and negative ion modes, scanning from *m*/*z* 80 to 1500 in 1 s. Cone voltages of 30 (negative ion) or 35 V (positive ion) and 70 V (both modes) were employed. Data were acquired by both the Masslynx data system for the mass spectrometer and the Beckman data system for the diode array; two wavelengths, 280 and 520 nm, from the diode array were also recorded by the Masslynx system to allow alignment of the data.

Nuclear Magnetic Resonance Spectrometry. NMR data were acquired on a Bruker DMX600 NMR spectrometer operating at a frequency of 600.18 MHz at 25 °C using TopSpin (version 1.3, Bruker GmbH). Samples were prepared in d_6-DMSO (99.98%; Sigma-Aldrich) in Shigemi tubes (Sigma-Aldrich) and degassed (argon) before sealing.

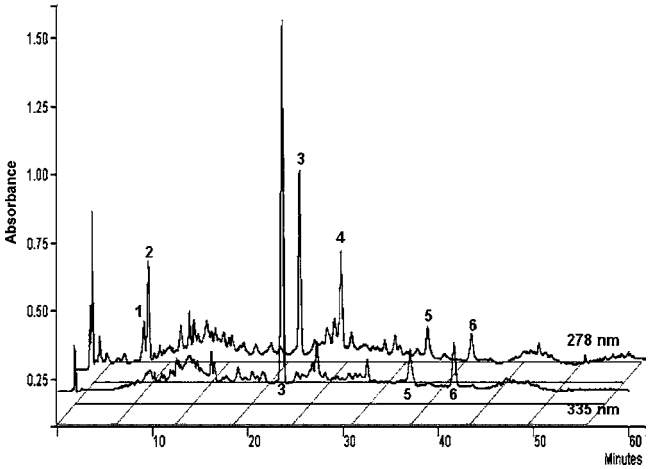

Figure 1. Reverse phase HPLC profile of crude hexane-washed OMW hydroalcoholic extract using analytical-scale conditions except for detection at 278 and 335 nm. Peaks: (1) hydroxytyrosol glucoside; (2) hydroxytyrosol; (3) verbascoside; (4) compound **A**; (5) compound **B**; (6) luteolin.

Spectral widths were set to allow at least 0.5 ppm on either side of observed resonances. 1D NMR spectra were recorded (6009.62 Hz) with 32K data points zero filled to 64K and resolution enhanced using a Gaussian multiplication of the raw FID (Gaussian broadening = 0.2, line broadening = −2 Hz) before Fourier transformation. All 2D NMR experiments were run with quadrature detection with a ^{1}H spectral width of 6009 Hz and a recycle delay of 2 s. Chemical shifts were referenced to the residual d_5-DMSO (δH 2.49; δC 39.8). High-power ^{1}H $\pi/2$ pulses were determined to be 10.0 μs and low power (for MLEV spin lock) at 25 ms. The ^{13}C high-power $\pi/2$ pulse was 11.0 μs, and a low-power pulse of 65 μs was used for GARP4 decoupling. Gradient pulses were delivered along the *z*-axis using a 100-step sine program.

Homonuclear proton−proton correlation was achieved with the eCOSY sequence (*10*) using gradient pulses for selection. The data were recorded in 4K data points in *t*2 and 512 data points in *t*1. Points were predicted out to 8K data points in *t*2 and 1K data points in *t*1 (maximum entropy) and zero filled to 8K and 4K data points, respectively. The data were processed using a $\pi/2$ sine-bell shifted apodization in both dimensions and carefully phase corrected. TOCSY experiments were recorded over 2K data points in *t*2 and 512 in *t*1 using the X_M16 sequence (*11*) for the mixing time (30 ms; P29 = 50 ms, SP0 = 8.86 dB). The data were processed using a $\pi/2$ sine-bell shifted apodization in both dimensions. HSQC spectra were recorded over 2K data points in *t*2 and 512 data points in *t*1 (10−170 ppm) using the sensitivity-enhanced double INEPT transfer with no trim pulses and adiabatic pulses for ^{13}C decoupling in *f*2 (*12*). The spectra were made phase sensitive using echo−antiecho gradient selection (80:20:11:−5). Long-range ^{1}H−^{13}C correlation (HMBC) spectra were recorded with 2K data points in *t*1 (10−210 ppm) and *t*2 and processed with magnitude calculation in *f*1 to destroy all phase information. Spectra were obtained with a low-pass *J* filter (145 Hz) to suppress one-bond correlations. No decoupling was used during the acquisition, and gradient pulses (50:30:40.1) were used for selection. Two experiments were run, optimized for 20 and 5 Hz long-range couplings, respectively. Long-range heteronuclear couplings were quantified with the J-HMBC experiment (*13*) using heteronuclear zero and double-quantum coherence for determination of long-range coupling constants (optimized for 2.5 Hz) by the splitting in *f*1 (scaled by 5×). Phase-sensitive acquisition was achieved using echo−antiecho gradient selection, and one-bond coupling (130−160 Hz) was suppressed using a 2-fold low-pass *J*-filter. Through-space connectivities were obtained using 2D homonuclear correlation via dipolar coupling (NOESY) using phase-sensitive echo−antiecho gradient selection with a 250 ms mixing delay (2K × 512 data points).

Free Radical Scavenging Activity. DPPH radical scavenging activity was evaluated according to the method of Kulisic et al. (*14*) with minor modification as follows. A stock methanolic solution of DPPH radical (32 mg/100 mL), prepared daily, was diluted 10-fold

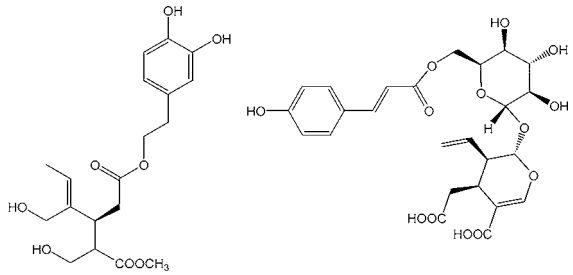

Figure 2. Chemical structures for compounds **A** and **B**.

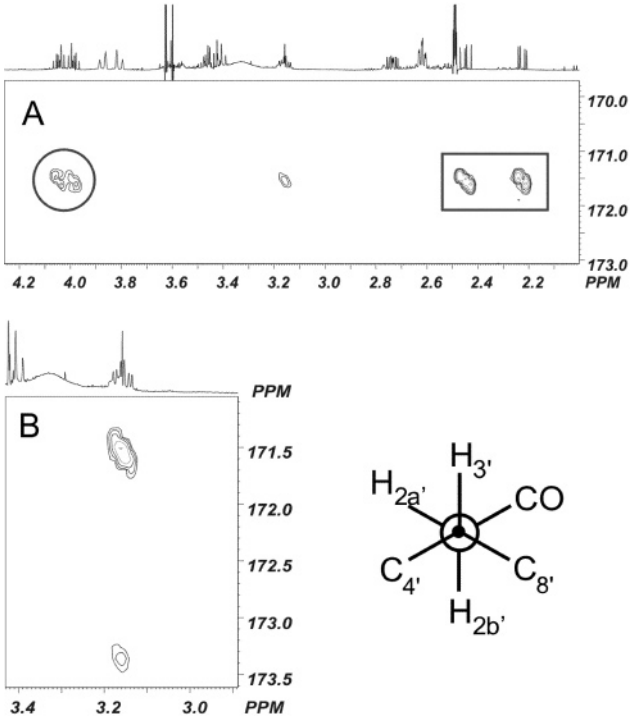

Figure 3. HMBC spectrum of compound **A** showing the key correlations connecting the phenylethanol and dihydroelenolic acid groups and a Newman projection for the C2′−C3′ bond as determined by measuring homonuclear and heteronuclear ^3J coupling constants. Panel **A** shows an expansion of the correlations of C1′ and panel **B** those of H3′.

with 80% aqueous methanol prior to use. Various concentrations of test samples in 80% aqueous methanol (200 μL) were added to 3 mL of the DPPH solution in plastic macrocuvettes (1 cm). The macrocuvettes were covered, well shaken, and kept in the dark for 1 h, and the absorbance was then measured at 517 nm. The percentage scavenging of DPPH radical was calculated according to the formula

$$\% \text{ scavenging} = 100 \times (A_{\text{control}} - A_{\text{sample}})/A_{\text{control}}$$

Statistical Analysis. All analyses were performed at least in triplicate. Data are expressed as means ± SD. Student's *t* test was used to test significant differences. For antioxidant activity, concentrations that resulted in 50% scavenging (EC_{50}) were calculated from the dose−response curves fitted to data points using Microsoft Excel software (*15*).

RESULTS AND DISCUSSION

HPLC chromatograms of the crude OMW extract exhibited six major peaks (**Figure 1**). These comprised four previously identified compounds, hydroxytyrosol glucoside, hydroxytyrosol, verbascoside, and luteolin (*8*), plus two compounds not previously reported in OMW. The former were identified on the basis of retention data and mass spectra by comparison with appropriate standards. The latter were designated compounds **A** and **B** and had retention times of 27.0 and 36.3 min, respectively. Compounds **A** and **B** were unidentified in our previous work (*8*).

Compound **A**, molecular weight of 382 (M − H^- 381 amu), was the most abundant biophenol in the waste (and fruit), although this is not apparent from chromatograms generated at 278 nm due to the relatively weak absorption of this compound at this wavelength. Nevertheless, it exhibited absorption maxima at 219 and 279 nm in the UV−vis spectrum, suggesting a catechol group was present (*16*). Proton NMR data showed a 1,3,4-trisubstituted benzene (2 × d, J = 8 Hz; 1 × singlet) consistent with hydroxytyrosol. The ethyl group (C7−C8) was evident from the HMBC spectrum, which showed $(H7)_2$ was coupled to C2 (δ_C 116.5), C6 (δ_C 119.9), and C1 (δ_C 128.5), whereas $(H8)_2$ was coupled only to C1 in the aromatic ring. The other half of the molecule contained an iridoid type moiety with a methyl ester [δ_C 174.9 (s), 51.6 (q)], two methenol groups [δ_C 61.9 (t), 62.7 (t)], and a propenyl group [δ_C 137.9 (s), 123.3 (d), 13.0 (q)]. The assignment of the H2′−H5′ spin group was straightforward using the eCOSY spectrum. The attachment of the carbomethoxy group at C3′ was indicated by the HMBC spectrum that showed correlations between C11′ and H3′, H4′, and H5′. H3′ additionally showed strong correlations to C8 and C9 and a weak correlation with C10 as did the H7′. This arrangement could be accommodated only with a dihydroelenolate moiety, either cyclic or acyclic. As the mass spectrum indicated a molecular weight of 382, this would correspond to a molecular formula of $C_{19}H_{26}O_8$, which has only seven degrees of unsaturation, consistent with an aromatic ring, two carbonyls, and the propenyl, so the iridoid moiety must be an acyclodihydroelenolate. The critical HMBC correlations tying the two components of compound **A** (**Figure 2**) together to yield the final structure (**1**) as shown in **Figure 3A** were the correlations between $(H8)_2$ of the tyrosol (circle) and $(H2')_2$ of the elenolate (rectangle) with C1′. The centrality of C3′ was also confirmed by the HMBC spectrum (**Figure 3B**), where H3′ showed $^3J_{CH}$ coupling to both carbonyl groups (C1′ and C11′). The stereochemistry indicated for **1** was on the basis of biogenetic considerations, where the dihydroelenolate would have originated from secologanin. The conformation about the C2′−C3′ bond was investigated using a J-HMBC spectrum and homonuclear couplings. H2a′ (δ_H 2.22) and H2b′ (δ_H 2.45) were coupled to each other by 15 Hz (π-assisted) and H2a′ to H3′ by 10.6 Hz, indicating an anti orientation. Consequently, H2b′ and H3 should be syn to each other, and this was confirmed by a small coupling ($^3J_{HH}$ = 4.5 Hz). The relative orientations of C4′ and C8′ were clear from the J-HMBC spectra, which indicated a 6.5 Hz coupling between H2a′ and C8′ and only 3.8 Hz between H2b′ and C8′. Similarly, a syn relationship between H2a′ and H2b′ with C4′ was indicated by couplings of 3.7 and 3.8 Hz, respectively, leading to the Newman projection in **Figure 3**. The stereochemistry at C4′ was not possible to ascertain through NMR spectroscopy because H3′ and H4′ were anti to each other and there were no differentiating $^3J_{CH}$ couplings. On the basis of these data the structure of compound **A** was tentatively assigned as 2-(3′,4′-dihydroxyphenyl)ethyl-4-(hydroxymethyl)-3-[2-(methyl-3-hydroxypropanoate)]-4-hexenoate (trivial name: hydroxytyrosyl acyclodihydroelenolate).

The UV spectrum of compound **B** (λ_{max} 225, 309 nm) suggested a *p*-coumaric acid derivative, confirmed by proton

Table 1. NMR Chemical Shift Data for Compounds **A** and **B** in d_6-DMSO (600 MHz)

	compound **A** hydroxytyrosol		compound **B** coumaric acid		
	^{13}C	^{1}H	^{13}C	^{1}H	^{13}C[a]
C1	128.8		125.2		127.6
C2	116.5	6.60 (d)	131.0	7.54 (d)	131.7
C3	145.5		115.7	6.40 (d)	117.3
C4	144.1		160.3		150.2
C5	116.6	6.55 (d)	115.7	6.40 (d)	117.3
C6	119.9	6.45 (dd)	131.0		131.7
C7	34.5	2.65 (dt)	145.2	7.53 (d)	147.4
C8	65.2	4.00/3.99 (m)	114.3	6.77 (d)	115.4
CO			167.0		168.8
			glucose		
C1′			99.3	4.55 (d)	100.6
C2′			72.6	3.02 (m)	75.0
C3′			76.3	3.18 (t)	78.3
C4′			69.5	3.15	72.1
C5′			73.8	3.43	76.2
C6′			63.5	4.37 (d), 4.22 (dd)	64.9
iridoid group			iridoid group		
C1	171.6		173		176.7
C2	36.1	2.45 (dd)/2.22 (dd)	34.0	2.80 (bd)/2.04 (dd)	35.5
C3	35.0	3.15 (dt)	27.2	3.03 (m)	154.0
C4	51.5	2.75 (ddd)	110.0		110.7
C5	61.9	3.45/3.41 (m)	150.7	7.34 (s)	154.0
O6					
C7	62.7	3.86 (d)/3.81 (d)	96.3	5.22 (d)	98.2
C8	137.9		43.1	2.64 (m)	45.7
C9	123.3	5.53 (q)	133.5	5.50 (dt)	134.9
C10	13.0	1.55 (d)	119.5	5.16 (d)/5.08 (d)	121.0
C11	174.9		168.5		169.6
OMe	51.6	3.72 (s)			

[a] Values for compound **B** (d_4-methanol) taken from ref *19*.

Table 2. Recovery Data, UV Spectral Data, and DPPH Antioxidant Scavenging Activity of Compounds **A** and **B**

	recovery[a] (mg/kg of freeze-dried OMW)	absorption maxima (nm)	DPPH scavenging activity, EC_{50} (μM)
hydroxytyrosol	NA	220 and 277	15.2 ± 0.8
oleuropein	NA	228 and 278	14.0 ± 0.1
compound **A**	3460 ± 200[b]	219 and 279	12.6 ± 0.3
compound **B**	120 ± 8[c]	225 and 309	24.3 ± 1.1

[a] Recoveries based on chromatographic peak areas and expressed as mean ± standard deviation for triplicate analyses. [b] Expressed as oleuropein equivalent. [c] Expressed as *p*-coumaric acid equivalent

NMR spectroscopy, which showed an aromatic AB system (δ_H 6.40, 7.54; $J = 8$ Hz) and a *trans*-double bond (δ_H 7.53, 6.77; $J = 16$ Hz). The olefinic protons (H7 and H8) were both coupled to a δ,β-unsaturated ester (δ_C 167.0) in the HMBC spectra. In the TOCSY spectrum there appeared to be a seven-proton spin system typical of a hexose. The ^{13}C NMR resonances of the hexose are in good agreement with published data for β-D-glucopyranosides (*17*) (**Table 1**). The anomeric proton at 4.55 ppm has a large coupling ($^3J_{HH} = 8$ Hz) to H2′, indicating both are axial. Additionally, large couplings between the other saccharide protons indicated a glucose nucleus. The remaining component contained a terminal olefin [δ_C 119.5(t)], immediately suggesting secologanic acid (*18*). The points of attachment between the three groups were elucidated with the aid of the HMBC spectrum (optimized for 20 Hz coupling). **Figure 4A** shows the HMBC correlations between the anomeric proton (H1′; 4.55 ppm) and C7″ of the secologanic acid residue and the correlation between H7″ (5.22 ppm) and the anomeric carbon (C1′; 99.3 ppm). Similarly, the coumaric acid carbonyl was coupled to both $(H6')_2$ protons of the glucose, confirming a 1,6-connection between the coumaric and secologanic acids, respectively. The NMR data agree fairly well with the published data despite the solvent being different (d_4-methanol) except for C4, which is more than 10 ppm different. As the chemical shifts of caffeoyl residues are well-known (*20*) and agree with our assignment, it is likely that the chemical shift reported by Karioti et al. (*19*) for C4 is in error. On the basis of NMR data, the structure of compound **B** is assigned as *p*-coumaroyl-6′-secologanoside (trivial name: comselogoside) (**Figure 2**).

Mass Spectra. ESI scans made at 30 or 35 V provided soft ionization conditions and confirmed the molecular masses for hydroxytyrosyl acyclodihydroelenolate and comselogoside (*21*) as 382 and 536 amu, respectively. Reconstructed mass chromatograms of the OMW generated at relevant *m*/*z* values corresponding to the pseudomolecular ions showed a single major peak in both positive and negative ion modes (data not shown). ESI at higher cone voltage of 70 V (**Figure 5**) provided

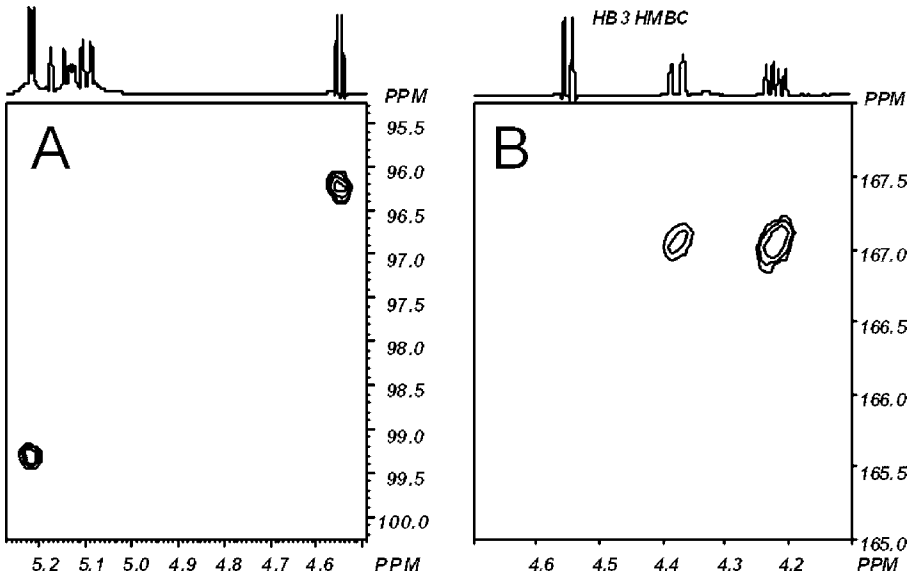

Figure 4. HMBC spectrum of compound **B** showing the key correlations connecting the coumaric (**A**) and secologanic (**B**) acids to the central glucose moiety.

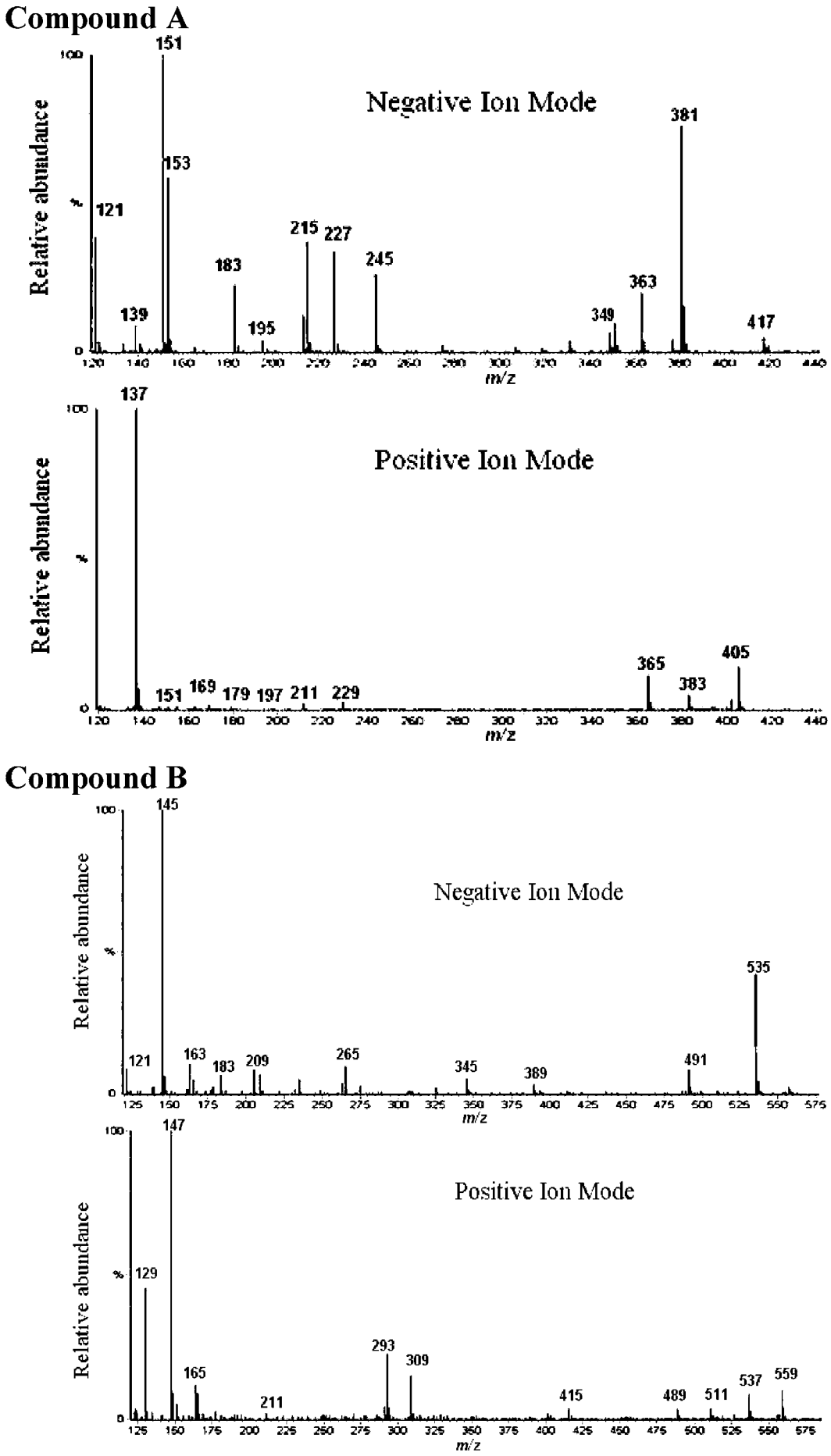

Figure 5. ESI mass spectra of compounds **A** and **B** at a cone voltage of 70 V.

fragmentation behavior. A notable feature is the relatively strong pseudomolecular ion for both compounds in negative ion mode.

General Comments. Hydroxytyrosyl acyclodihydroelenolate has not previously been identified. To the best of our knowledge this is the first reported example of a nonaldehydic open cycle secoiridoid in olives.

We previously noted the occurrence of comselogoside in OMW (*8*) but did not assign a structure at that stage. Since the completion of this work, comselogoside has been reported in olive leaf associated with growth under stressed conditions of boron deficiency (*19*). Under these conditions oxidative damage accumulates in cells, and production of compounds with antioxidant activity may be a useful strategy to minimize oxidative damage.

Both hydroxytyrosyl acyclodihydroelenolate and comselogoside exhibited in vitro DPPH$^{\bullet}$ scavenging ability comparable to that of more recognized antioxidants (**Table 2**). DPPH$^{\bullet}$ is a long-lived radical that is extensively used for primary screening of antioxidant activity of plant extracts and phytochemicals (*9*). DPPH radical scavenging assay correlates well with lipid peroxidation, LDL oxidation (*22*), and cytotoxic activity (*23*) and is useful for relative ranking of antioxidants, although extrapolation into in vivo systems should be avoided (*24*). Hydroxytyrosyl acyclodihydroelenolate was twice as active as comselogoside on a molar basis, consistent with the fact that catechols are more efficient antioxidants compared with monohydroxyphenols. Hydroxytyrosyl acyclodihydroelenolate was a more efficient radical scavenger than hydroxytyrosol and oleuropein. It appears that the linear structure of hydroxytyrosyl acyclodihydroelenolate makes it more accessible to the sterically hindered DPPH radical (*25*).

OMW continues to be a source of novel compounds with potential bioactivity. The discovery of compound **A** highlights the diverse range of degradation reactions of secoiridoid derivatives, with diol derivatives now added to the well-known dialdehyde compounds.

ACKNOWLEDGMENT

We thank Daniel Jardine, Flinders University, Adelaide, for assistance with LC-MS work.

LITERATURE CITED

(1) Owen, R. W.; Giacosa, A.; Hull, W. E.; Haubner, R.; Spiegelhalder, B.; Bartsch, H. The antioxidant/anticancer potential of phenolic compounds isolated from olive oil. *Eur. J. Cancer* **2000**, *36*, 1235−1247.

(2) Visioli, F.; Galli, C. Biological properties of olive oil phytochemicals. *Crit. Rev. Food Sci.* **2002**, *42*, 209−221.

(3) Obied, H. K.; Allen, M. S.; Bedgood, D. R.; Prenzler, P. D.; Robards, K.; Stockmann, R. Bioactivity and analysis of biophenols recovered from olive mill waste. *J. Agric. Food Chem.* **2005**, *53*, 823−837.

(4) Schieber, A.; Stintzing, F. C.; Carle, R. By-products of plant food processing as a source of functional compounds−recent developments. *Trends Food Sci. Technol.* **2001**, *12*, 401−413.

(5) Moure, A.; Cruz, J. M.; Franco, D.; Dominguez, J. M.; Sineiro, J.; Dominguez, H.; Jose, Nunez, M.; Parajo, J. C. Natural antioxidants from residual sources. *Food Chem.* **2001**, *72*, 145−171.

(6) Beauchamp, G. K.; Keast, R. S. J.; Morel, D.; Lin, J. M.; Pika, J.; Han, Q.; Lee, C. H.; Smith, A. B.; Breslin, P. A. S. Phytochemistry−ibuprofen-like activity in extra-virgin olive oil. *Nature* **2005**, *437*, 45−46.

(7) Rodis, P. S.; Karathanos, V. T.; Mantzavinou, A. Partitioning of olive oil antioxidants between oil and water phases. *J. Agric. Food Chem.* **2002**, *50*, 596−601.

(8) Obied, H. K.; Allen, M. S.; Bedgood, D. R.; Prenzler, P. D.; Robards, K. Investigation of Australian olive mill waste for recovery of biophenols. *J. Agric. Food Chem.* **2005**, *53*, 9911−9920.

(9) Roginsky, V.; Lissi, E. A. Review of methods to determine chain-breaking antioxidant activity in food. *Food Chem*. **2005**, *92*, 235−254.

(10) Griesinger, C.; Sorensen, O. W.; Ernst, R. R. Practical aspects of the E-COSY technique−measurement of scalar spin spin coupling-constants in peptides. *J. Magn. Reson.* **1987**, *75*, 474−492.

(11) Peti, W.; Griesinger, C.; Bermel, W. Adiabatic TOCSY for C, C and H, H J-transfer. *J. Biomol. NMR* **2000**, *18*, 199−205.

(12) Schleucher, J.; Schwendinger, M.; Sattler, M.; Schmidt, P.; Schedletzky, O.; Glaser, S. J.; Sorensen, O. W.; Griesinger, C. A general enhancement scheme in heteronuclear multidimensional NMR employing pulsed-field gradients. *J. Biomol. NMR* **1994**, *4*, 301−306.

(13) Meissner, A.; Sorensen, O. W. Measurement of *J*(H,H) and long-range *J*(X,H) coupling constants in small molecules. Broadband XLOC and J-HMBC. *Magn. Reson. Chem*. **2001**, *39*, 49−52.

(14) Kulisic, T.; Radonic, A.; Katalinic, V.; Milos, M. Use of different methods for testing antioxidative activity of oregano essential oil. *Food Chem.* **2004**, *85*, 633−640.

(15) Savelev, S.; Okello, E.; Perry, N. S. L.; Wilkins, R. M.; Perry, E. K. Synergistic and antagonistic interactions of anticholinesterase terpenoids in *Salvia lavandulaefolia* essential oil. *Pharmacol. Biochem. Behav.* **2003**, *75*, 661−668.

(16) Scott, A. I. *Interpretation of the Ultraviolet Spectra of Natural Products*; Pergamon: London, U.K., 1964.

(17) Bock, K.; Pedersen, C. Carbon-13 NMR spectroscopy of monosaccharides. *Adv. Carbohydr. Chem. Biochem.* **1983**, *41*, 27.

(18) Damtoft, S.; Franzyk, H.; Jensen, S. R. Biosynthesis of secoiridoids in fontanesia. *Phytochemistry* **1995**, *38*, 615−621.

(19) Karioti, A.; Chatzopoulou, A.; Bilia, A. R.; Liakopoulos, G.; Stavrianakou, S.; Skaltsa, H. Novel secoiridoid glucosides in *Olea europaea* leaves suffering from boron deficiency. *Biosci., Biotechnol., Biochem*. **2006**, *70*, 1898−1903.

(20) Wu, J.; Huang, J. S.; Xiao, Q.; Zhang, S.; Xiao, Z. H.; Li, Q. X.; Long, L. J.; Huang, L. M. Spectral assignments and reference data−complete assignments of H-1 and C-13 NMR data for 10 phenylethanoid glycosides. *Magn. Reson. Chem*. **2004**, *42*, 659−662.

(21) Innocenti, M.; La Marca, G.; Malvagia, S.; Giaccherini, C.; Vincieri, F. F.; Mulinacci, N. Electrospray ionisation tandem mass spectrometric investigation of phenylpropanoids and secoiridoids from solid olive residue. *Rapid Commun. Mass Spectrom*. **2006**, *20*, 2013−2022.

(22) Katsube, T.; Tabata, H.; Ohta, Y.; Yamasaki, Y.; Anuurad, E.; Shiwaku, K.; Yamane, Y. Screening for antioxidant activity in edible plant products: comparison of low-density lipoprotein oxidation assay, DPPH radical scavenging assay, and Folin−Ciocalteu assay. *J. Agric. Food Chem.* **2004**, *52*, 2391−2396.

(23) Rousseau-Richard, C.; Auclair, C.; Richard, C.; Martin, R. Free radical scavenging and cytotoxic properties in the ellipticine series. *Free Radical Biol. Med.* **1990**, *8*, 223−230.

(24) Rice-Evans, C. Methods to quantify antioxidant activity of tea/tea extracts *in vitro*. *Crit. Rev. Food Sci. Nutr*. **2001**, *41*, 405−406.

(25) Gordon, M. H.; Paiva-Martins, F.; Almeida, M. Antioxidant activity of hydroxytyrosol acetate compared with that of other olive oil polyphenols. *J. Agric. Food Chem.* **2001**, *49*, 2480−2485.

Received for review November 14, 2006. Revised manuscript received February 1, 2007. Accepted February 2, 2007. We thank Rural Industries Research and Development Corporation and CSU for financial support.

JF063300U